Int J Adv Manuf Technol (2010) 49:53–62
DOI 10.1007/s00170-009-2382-3

ORIGINAL ARTICLE

Surface quality in milling of hardened H13 steel

Gerson L. Nicola · Frank P. Missell · Rodrigo P. Zeilmann

Received: 27 April 2009 / Accepted: 14 October 2009 / Published online: 29 October 2009

Abstract In the final milling process of free-form surfaces, commonly employed in the production of molds and dies, knowledge of the cutting conditions and a strategy for choosing adequate processing routes can provide a significant reduction in the manufacturing times. The objective of this work is to evaluate quantitatively and qualitatively the surface quality behavior of a steel used in the production of dies and molds. The analysis was carried out for hardened AISI H13 tool steel inclined at an angle of 60° and for different cutting path orientations. The roughness of milled surfaces was measured and verified by scanning electron microscopy in order to compare the strategies and the surface textures obtained. Four different cutting path strategies were employed in these experiments, with horizontal and vertical single-direction rastering, both upward and downward. The conclusion is that, in the vertical upward strategy, the surface displays greater roughness and an irregularity with regard to plastic deformation. The other strategies showed lower roughness and similar regularity. Magnetic Barkhausen noise, used for sub-surface characterization, was found to be largest when measured along the cutting direction of the inserts. These directions coincided with the directions of greatest plastic deformation in the sub-surface region.

Keywords Cutting path · Surface texture · Hardened H13 steel · Ball-end milling · Magnetic Barkhausen noise

G. L. Nicola · F. P. Missell · R. P. Zeilmann (✉)
Department of Mechanical Engineering, CCET,
University of Caxias do Sul,
Caxias do Sul, Rio Grande do Sul 95070-560, Brazil
e-mail: rpzeilma@ucs.br

1 Introduction

Progress and advancement in technologies such as the design of molds and die cavities, cutting tools, machine tool design, and computational systems for design and manufacture (computer-aided design/computer-aided manufacturing (CAD/CAM)) have made possible the machining of hardened materials. A practical result is that it offers advantages in the processing and in the final machined product, providing good surface quality and dimensional control as shown by Junz Wang and Zheng [1]. In the final milling process of free surfaces with complex geometries, knowledge of the cutting conditions and the choice of adequate processing may provide a significant reduction in the manufacture times. Machines equipped with computer numerical control (CNC) have the movements of their axes and trajectories defined by a programmer. The surface of a machined piece is composed of many texture components, which are generated during the manufacturing process. The milling process produces a pattern of regular and repetitive ridges, with a clearly visible preferential direction defined by these ridges [2]. Knowledge of the recommended machining strategy for a specific condition, as well as the finishing of the surface obtained, can be of great value for the programmers in the defining phase of the process.

Although the machining of hardened steels presents difficulties during machining, Junz Wang and Zheng [1] showed that it offers advantages in the process and the final machined product, providing improvement in surface quality and dimensional control. A final machining after the thermal treatment, with the material already at the final work hardness, prevents recurrent problems related to the hardness, such as possible workpiece distortion and dimensional variation.

One of the more basic and predominant geometric forms in the manufacture of molds and die cavities is the inclined plane. To simulate a finishing condition, a geometry of low complexity was adopted, defined as an inclined surface, in one workpiece of definite and reduced dimensions. The main doubt in the machining of this geometry is to know what the best strategy is, defined as the tool trajectory. This includes the workpiece inclination, defined as the angle formed between the tool and a plane normal to the axis of the tool. We consider the ball-nose end mill, which is the type of tool most appropriate for finishing processes on surfaces with complex forms. In the literature, studies of the machining of inclined planes are restricted mainly to evaluating the life of the tool and varying the cutting conditions (feeds and speeds). A smaller number of papers go beyond this and consider the cutting strategies, comparing them with the surface quality obtained. The strategies are defined by the feed and cutting directions, being vertical or horizontal with respect to the plane, and with a direction that can be ascending (upward) or descending (downward).

According to Tabenkin [3], the finishing or texture can be described in terms of the number and direction of the valleys and peaks that compose a surface. The analysis of the surface, in practical terms, can be made in terms of three basic components: roughness, undulation, and form. Generally, the three exist simultaneously, overlapping, although in many situations, it is desirable to examine each condition independently. In general, it can be said that the roughness has a shorter wavelength than the undulation, which, in turn, has a shorter wavelength than the form shunting line. In the milling process, the cutting edges of the tool have a motion that is a combination of translation and rotation. The periodic variation of the cutting edge orientation during spindle rotation results in two kinds of scallops being generated on the machined surface: the pick-interval and the feed-interval scallops [4].

Chen et al. [4] presented a new model that describes the path-interval and feed-interval scallops generated in the ball-end milling processes. They claimed that the scallop height was continuously reduced by increasing the tool-axis inclination angle. An inclination angle up to 10 degrees is, however, good enough for most tool diameters from the surface roughness viewpoint.

Kang et al. [5] carried out a comparative study, evaluating the characteristics of machined steel with a hardness of 28 HRc in a workpiece of planar geometry, varying the angle of inclination to 15, 30, and 45 degrees, using four possible cutting strategies. They used a solid carbide ball nose end mill coated with TiAlN, having a diameter of 10 mm and two cutting edges. They presented a qualitative and quantitative analysis of the surfaces obtained, showing images of the surface texture and graphs of roughness for each condition. The texture obtained for each condition shows the influence of the cutting strategy employed. These authors reported that the strategies employing an ascending cut, with the tool executing the cut from the base of the inclined plane and going up, presented lower values of surface roughness and a more homogeneous texture when compared with the descending strategies.

Toh [6] carried out an analysis of the topography of surfaces machined on AISI H13 with hardness 52 HRc. The analysis evaluated different cutting strategies and cutting path orientations, using a planar geometry, inclined at 75°, simulating a finishing process. They used a solid tungsten carbide ball nose end mill, with TiAlN coating, with a diameter of 10 mm and six cutting edges. The objective was to understand the surface texture generated by certain cutting path orientations in a material of difficult machinability. An analysis of the topography resulted in three-dimensional graphs of the roughness profile and allowed a determination of the best orientation for obtaining texture of better quality. In conclusion, Toh reported that the strategy involving an ascending vertical cut provided the best results.

In general, it is very difficult to try to represent the diverse variables involved in the formation of complex surfaces generated by the milling process. The result of milling is strongly influenced by the dynamic behavior, which depends upon the cutting parameters, as well as the contact between the cutting tool and the workpiece. Small alterations in the system can be magnified in the dynamic behavior, affecting results, especially the surface quality. The challenge is to plan experiments that cover representative situations to obtain results that really contribute to an understanding of the process and its variables.

The objective of this study is to analyze the surface quality produced on hardened hot worked AISI H13 die steel by the end milling process, using an inclined workpiece angle of 60 degrees in relation to the horizontal plane, with different cutter path orientations. For this present study, the ball-nose end mill was used with an indexable insert, as commonly used in the mold and die industry. This type of tool is frequently used in finishing processes, mainly because of the cost reduction obtained for the case of large surfaces.

2 Experimental work

2.1 Workpiece and tool

Hardened AISI H13 hot worked tool steel with a chemical composition of 0.4% C, 0.94% Si, 0.36% Mn, 5.04% Cr, 1.22% Mo, and 0.88% V, according to the quality

certificate of Gerdau Aços Finos Piratini (2005), was used throughout the experimental work. This steel is frequently used in the manufacture of molds and die cavities. The workpiece was hardened and annealed to obtain a final hardness of 54 HRc. The workpiece material was machined into blocks with dimensions of 50 × 50 × 25 mm. Normally, the cavities machined in molds and dies have a complex geometry. However, for laboratory experiments, it would be very complicated to try to represent all of the usual cavity geometries. Thus, we have chosen to use workpieces that facilitate the experiments and have chosen a representative case for the tool/workpiece orientation.

The tool used in these experiments was an indexable insert tungsten carbide, ball-nose end mill, ISO H10 class, with TiAlN PVD coating, indicated for the final milling of hard steel. The cutter has a nominal diameter of 16 mm and two cutting edges (z), with a clearance angle of 13° and a null rake angle. The cylindrical tool shank is made up of steel, fixed in a Weldon tool-holding system. All machining experiments were performed on a Dyna DM 4500 vertical Machining Centre, with maximum rotation of 6,000 rpm and power of 7.5 kW.

2.2 Characterization equipment

For the roughness measurements of the machined surfaces, a Veeco Dektak 6 M bench-top surface profiler was used, with Dektak 6 M software and a high-resolution 0.7-μm-radius sub-micron stylus, located at the Division of Materials Metrology of INMETRO. Using a 2D surface stylus instrument, the parameters that characterize surface roughness can be easily determined and quantified. For the visualization of the surface texture, a FEI Quanta 200 scanning electron microscope (SEM) was used at the Division of Materials Metrology of INMETRO. The main advantage of using the SEM is that real-life surface characterization can be performed more reliably.

Measurements of the rms Barkhausen noise (BN) voltage were made using a Rollscan 300 from Stresstech. The magnetizing frequency employed was 125 Hz and the analyzing filter passed BN frequencies in the range 70–200 kHz.

2.3 Experimental procedure

The effect of employing different cutting path orientations, when machining hardened AISI H13, was investigated in relation to workpiece surface roughness. Figure 1 illustrates the cutting path orientations employed in this work. Four cutting strategies were considered, as defined by the trajectory of the tool, with climb cut only, upward and downward, in the horizontal and vertical directions. For the climbing direction, the cutter moves in parallel lines scanning across the area to be machined. The cutter mills across the machined surface, steps over a fixed amount, and moves back to the original position through the air before milling across another line.

The strategies implemented and the CNC cutting paths were defined using Unigraphics NX4 CAM software. For each strategy, the machined area was limited to 20 × 50 mm on the workpiece face. The machined region, the initial machining point for each strategy, and the cutting path orientations for the pick feed direction (a_e) and the feed direction (f_z) are illustrated in Fig. 2.

For each test, one new cutting edge was used after having been previously checked. All machining tests were conducted dry. In addition, a blast of compressed air was delivered through a nozzle to the tool to facilitate the chip removal. The workpiece was fixed on a device with an inclination of 60 degrees in relation to the horizontal plane, as illustrated in Fig. 3.

Cutting parameters were chosen based upon preliminary tests developed in the laboratory to evaluate stability conditions, which could reduce the influence of vibrations due to the inclination of the workpiece. In Table 1, we present the machining conditions used in the preliminary tests.

Based on the results presented in Table 2, the cutting speed (v_c) and feed per tooth (f_z) were chosen and used for all the strategies considered, as shown in Table 3. The average value of the effective cutting diameter was adopted and calculated for the upward and downward strategies. The tool overhang, defined for the length of tool until the tool holder, was kept the same for all the tests, being fixed at 2.5 times the value of the nominal diameter of the tool.

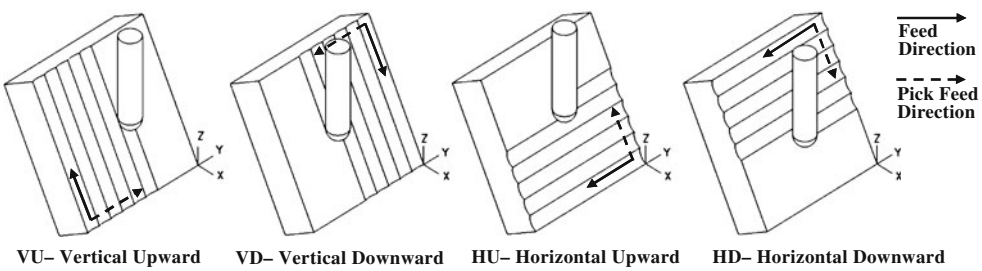

Fig. 1 Cutting path orientations considered here

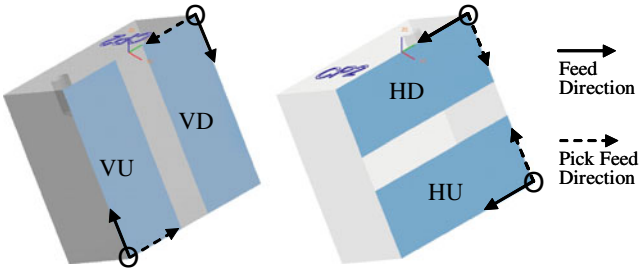

Fig. 2 Machined regions of workpiece and cutting path orientations

Table 1 Cutting parameters used in the preliminary tests

Parameters	Trial A	Trial B	Trial C	Trial D
Tool diameter (mm)	13.51	13.51	13.51	13.51
v_c (m/min)	150	150	180	180
a_p (mm)	0.2	0.2	0.2	0.2
a_e (mm)	0.2	0.1	0.2	0.1
f_z (mm)	0.1	0.1	0.1	0.1
Rotation (rpm)	3,534	3,534	4,241	4,241

3 Results and discussion

The workpiece surface roughness was measured using the contact stylus, which was moved along the feed direction (f) and the pick feed direction (a_e). The average parameters Ra and R_{z_DIN} were adopted to characterize the workpiece surface roughness, where Ra is the arithmetic average in the measured segment and R_{z_DIN} represents the average of the maximum roughness over five measurement intervals. A sampling length of 2.0 mm and a cut-off length of 0.4 mm were employed. The final average roughness values are given in Table 4. For measurement, the stylus was positioned onto the initial track of the tool, parallel to the feed and pick feed directions.

In Figs. 4 and 5, graphs of surface roughness are shown that had been generated from data obtained with the VEECO Dektak 6 M software. The graphs represent the roughness in the feed direction (f_z) and the pick feed direction (a_e), on the same measurement scale.

These two figures reinforce the message of Table 4 and clearly illustrate how the machined surface obtained from the vertical upward strategy (VU) presented the largest roughness values in both directions evaluated. This effect occurred for all repetitions with the same strategy. The tool wear after the tests was not significant, indicating that the texture results from mechanical contact. That is, the texture results from an inability to maintain the cutting edge in permanent contact with the formed surface.

Figures 6, 8, 9, and 10 show secondary electron SEM images of the textures obtained, with magnifications varying from 50× up to 500×. The surface roughness can be easily visualized with SEM, and it is possible to see clearly that the textures that result from surface machining show the influence of the cutting strategy employed.

Figure 6 shows surface texture resulting from the VU strategy. An irregular texture is verified, which the marks and scallops generated in machining had not clearly revealed. For this condition, the worst surface texture is observed. For higher magnifications especially (Fig. 6 with magnification of 500×), material adhesion on the machined surface is clearly seen. This was an important contribution towards a substantial increase in the roughness for this strategy. Toh [6] found the VU orientation to give the best workpiece surface texture for a 75° inclination. However, Toh used a solid tungsten carbide ball-nose end mill, having a TiAlN coating and a diameter of 10 mm, with six cutting edges, especially made for his experiment. According to Toh, the worst surface texture resulted from the vertical downward orientation. Kang et al. [5] and Ng et al. [7] also reported that the vertical downward orientation at an inclined workpiece angle of 45◦ gave the worst surface finish. This was attributed to the high tendency for cutter vibration. In contrast, the findings of Tonshoff and Camacho [8] suggested that vertical downward orientation gave a better surface finish because the majority of the cutting forces were transmitted to the cutter axis.

Returning now to the material adhesion clearly seen in Fig. 6, it is known that adhesion involves the transfer of electrons between the adhering surfaces. Thus, it is favored by a clean, oxide-free surface. The coefficient of friction between clean iron surfaces is very high, but it can be reduced substantially by allowing the formation of a thin oxide coating. Similarly, adhesion is favored on smooth surfaces. In the case of rough surfaces, the surface asperities

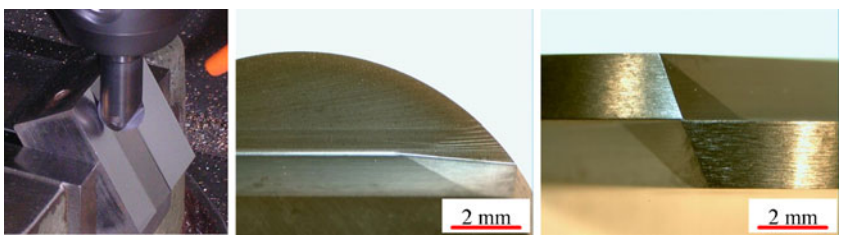

Fig. 3 Images of the test setup (*left*), tool face (*center*), and tool flank (*right*)

Table 2 Average roughness values (μm) from preliminary tests

Trial	Direction	AVERAGE ROUGHNESS VALUES											
		HU			HD			VU			VD		
		Ra	Ry	Rz	Ra	Ry	Rz	Ra	Ry	Rz	Ra	Ry	Rz
A	fz	0.24	1.31	0.93	0.18	1.10	0.71	0.43	3.43	2.34	0.39	2.33	1.70
	St.Dev.	0.04	0.12	0.18	0.04	0.31	0.27	0.03	0.14	0.14	0.09	0.57	0.40
	ae	0.33	2.26	1.58	0.86	2.70	2.30	0.46	2.70	1.77	0.35	1.79	1.26
	St.Dev.	0.04	0.17	0.10	0.59	0.12	0.08	0.05	0.29	0.21	0.03	0.12	0.13
B	fz	0.18	1.09	0.68	0.15	1.04	0.65	0.44	2.79	1.90	0.46	2.74	2.21
	St.Dev.	0.02	0.17	0.10	0.04	0.36	0.26	0.14	0.56	0.37	0.05	0.37	0.25
	ae	0.61	2.90	2.45	0.48	2.17	1.87	0.35	2.03	1.34	0.41	2.19	1.56
	St.Dev.	0.01	0.06	0.03	0.03	0.20	0.09	0.03	0.19	0.15	0.05	0.17	0.17
C	fz	0.27	1.45	0.98	0.20	0.99	0.71	1.46	7.50	5.12	0.57	2.95	2.62
	St.Dev.	0.05	0.24	0.14	0.04	0.17	0.14	0.10	0.26	0.16	0.06	0.25	0.13
	ae	0.62	3.08	2.51	0.32	2.29	1.84	0.88	5.20	3.42	0.31	1.48	0.98
	St.Dev.	0.02	0.06	0.01	0.01	0.11	0.05	0.12	0.64	0.37	0.02	0.08	0.08
D	fz	0.28	1.50	1.00	0.19	1.10	0.74	1.41	7.92	5.52	0.31	2.10	1.82
	St.Dev.	0.04	0.21	0.12	0.11	0.52	0.49	0.21	0.88	0.40	0.03	0.21	0.18
	ae	0.78	3.69	3.31	0.27	1.96	1.62	1.43	8.09	5.22	0.23	1.32	0.86
	St.Dev.	0.01	0.07	0.07	0.01	0.09	0.04	0.32	1.42	0.97	0.04	0.16	0.13

must be deformed in order for the contacting surfaces to come into close proximity. The adhesion is therefore strongly influenced by the size of the asperities. A relationship between adhesion and surface roughness was developed by Fuller and Tabor [9] for elastic solids many years ago. When the surface asperities undergo severe plastic deformation, as might occur during motion, the formation of transfer films or transfer particles frequently results. These transfer particles can result in the transfer of material from one surface to another and give rise to a wear mechanism, which can have undesirable consequences for the surface under consideration. The images of Fig. 6 are typical of adhesive wear [10] and suggest that a similar phenomenon may be occurring in the present case. The surface roughness observed in Fig. 6 may be the result of wear generated by heavily deformed transfer particles.

A different explanation, an alternative to that presented by Stachowiak and Batchelor [10], would be a mixed behavior having elements in common with both adhesive wear and an excessive plastic deformation occurring between the cutting edge of the tool and the machined surface. Figure 7 shows a schematic sequence of this type of wear, herein referred to as adhesive-deformation wear.

The process referred to would have its origin in adhering particles that would be deformed against the machined surface during the passage of the cutting tool. This passage results in a contact that is intense, but irregular. That is, there exists a certain oscillatory behavior in the contact between cutting edge/flank and the resulting surface. In this manner, part of the material that should be carried away to the tool extremity and expelled in the form of the chip is entering between the cutting edge and the workpiece surface, resulting in a highly deformed micro-layer that adheres to the final surface of the machined piece.

For the texture resulting from the vertical down (VD) strategy, shown in Fig. 8, square forms appear, with tracks and scallops resulting from the tool in the feed direction (f_z) and the pick feed direction (a_e) being clearly identified. The marks and scallops are repetitive and can be observed and quantified in the roughness graphs (Fig. 4c, d).

Figure 9 shows the surface texture resulting from the horizontal up (HU) strategy, where marks and scallops from the tool in the feed direction (f_z) and the pick feed direction (a_e) are clearly identified. The marks and scallops are repetitive and distinct for the feed and pick feed directions,

Table 3 Final cutting parameters employed

Average effective tool diameter—de (mm)	13.51
Tool overhang—l (mm)	40
Cutting speed—v_c (m/min)	150
Axial depth of cut—a_p (mm)	0.2
Pick feed—a_e (mm)	0.2
Feed per tooth—f_z (mm)	0.1
Spindle revolution—n (rpm)	3,534
Cutting edges—z	2
Machining time (min)	11.5

Table 4 Final values of measured surface roughness

Direction	Surface roughness (μm)							
	VU		VD		HU		HD	
	R_a	R_{z_DIN}	R_a	R_{z_DIN}	R_a	R_{z_DIN}	R_a	R_{z_DIN}
Feed	0.50	2.82	0.24	0.91	0.23	0.93	0.19	0.58
Pick feed	0.69	3.62	0.17	0.64	0.31	1.62	0.31	1.50

being observable and quantified in the roughness graphs (Fig. 5a, b). Marks of the tracks are clearly verified in the feed direction. A little material adhesion on the machined surface deposited alongside the feed marks was observed. For the VU strategy, the upward direction may have a higher linear speed of cutting than the downward direction. Differences in cutting characteristics also occur where the contact point of the ball-end mill changes, as on an inclined plane, because the effective tool diameter changes.

In the texture resulting from the horizontal down (HD) strategy, shown in Fig. 10, well-defined marks from the tracks are seen and are clearly verified in the feed direction (*f*). For this strategy, material adhesion side flow was not observed.

Magnetic Barkhausen noise (MBN) can also be used to characterize stress levels in surface and sub-surface regions of machined objects. A recent NPL Measurement Good Practice Guide by Buttle et al. [11] outlines magnetic measurement techniques for residual stress measurements. The orientation of the yoke of the MBN probe used to characterize our materials defines the direction of the applied magnetic field and allows one to sample stress levels along that direction. For the VU and VD machining strategies, the measured MBN was larger when measurements were made in the direction transverse to the tool feed (that is, in the a_e direction). For the HU and HD strategies, larger values of MBN were obtained for the direction of tool feed. Figure 11 illustrates this behavior graphically, showing average values of MBN along (f_z) and transverse (a_e) to the tool feed.

This result can be understood from an analysis of the cutting mechanism during milling, where the material removal occurs with the simultaneous rotation and translation of the cutting tool. During the milling of inclined surfaces, the cutting movement of the insert occurs in a direction transverse to the tool feed for the VU and VD strategies, whereas, for the HU and HD strategies, the cutting movement of the insert is along the tool feed. Thus, it appears that the largest values of MBN were encountered along the cutting direction of the insert, in all cases. This

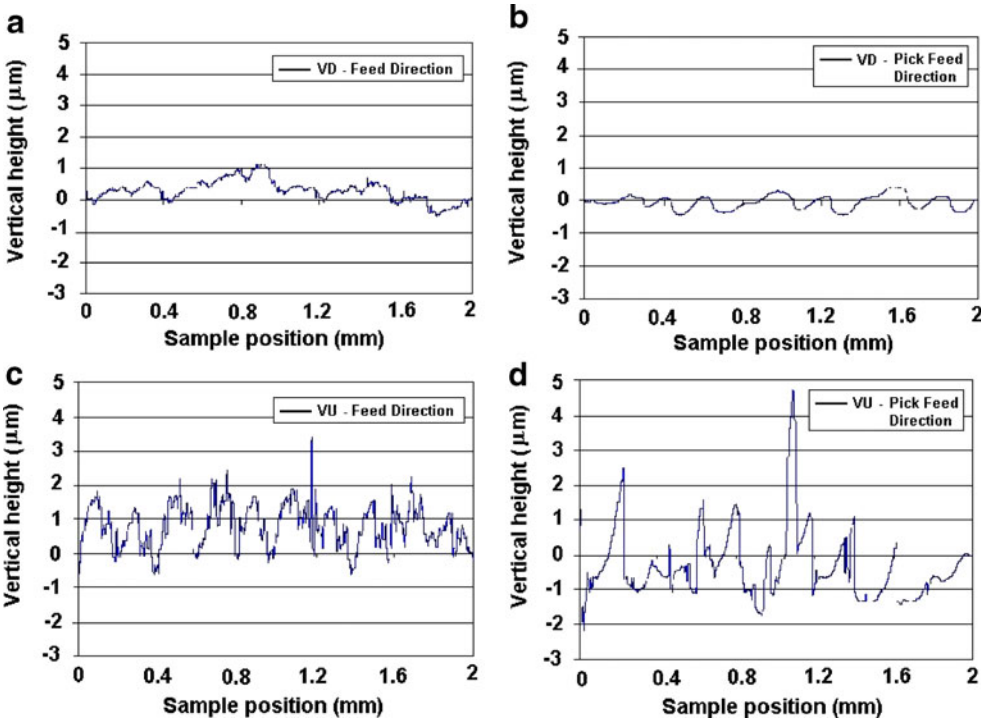

Fig. 4 Surface roughness for the VU (**a**, **b**) and VD (**c**, **d**) strategies

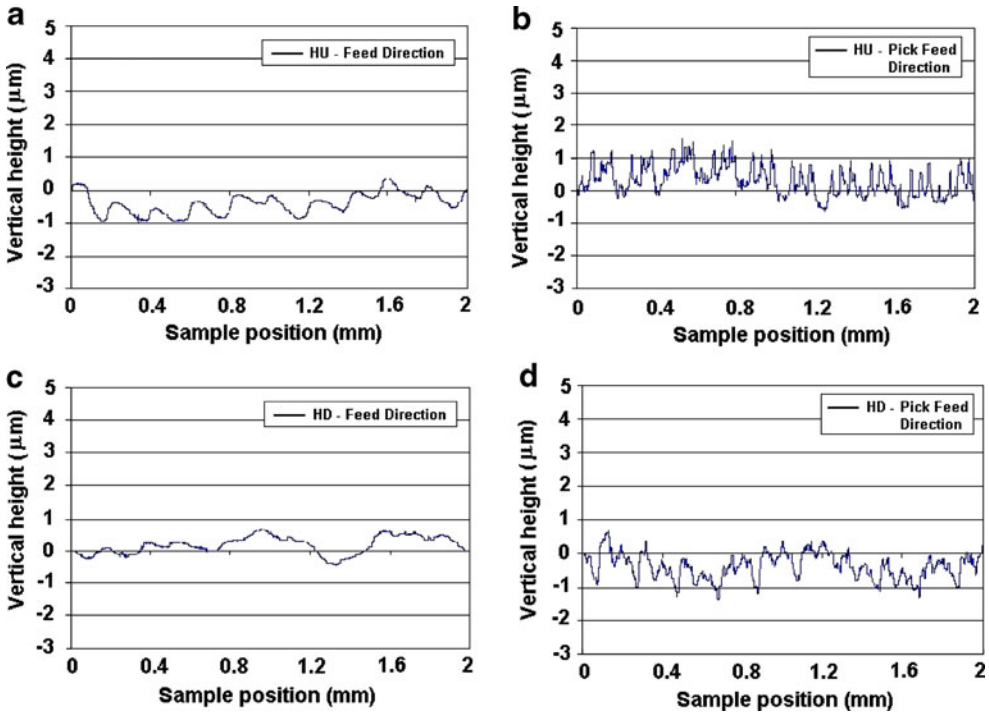

Fig. 5 Surface roughness for the HU (**a**, **b**) and HD (**c**, **d**) strategies

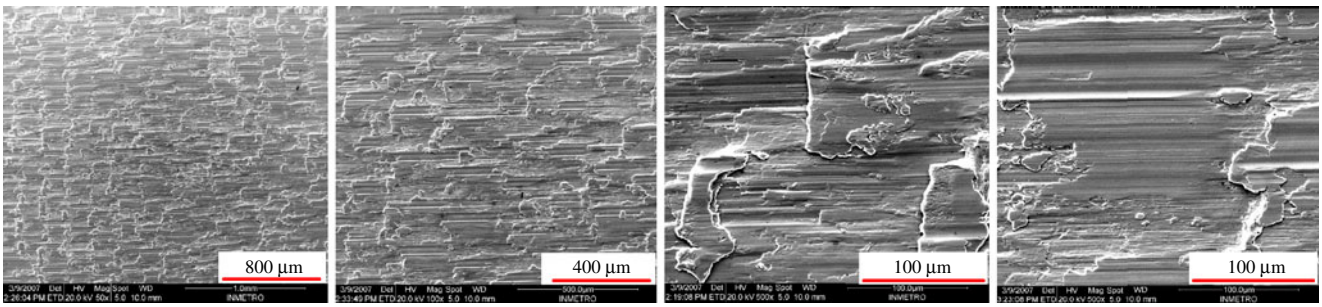

Fig. 6 SEM images for the VU strategy with magnifications (*left* to *right*) of 50×, 100×, 500×, and 500×

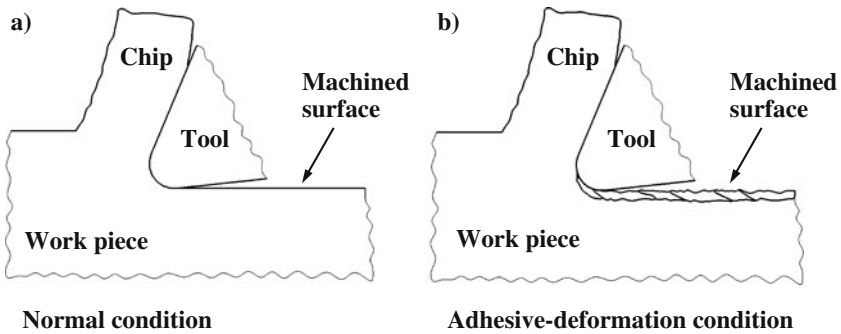

Fig. 7 Adhesive-deformation process (**a**, **b**)

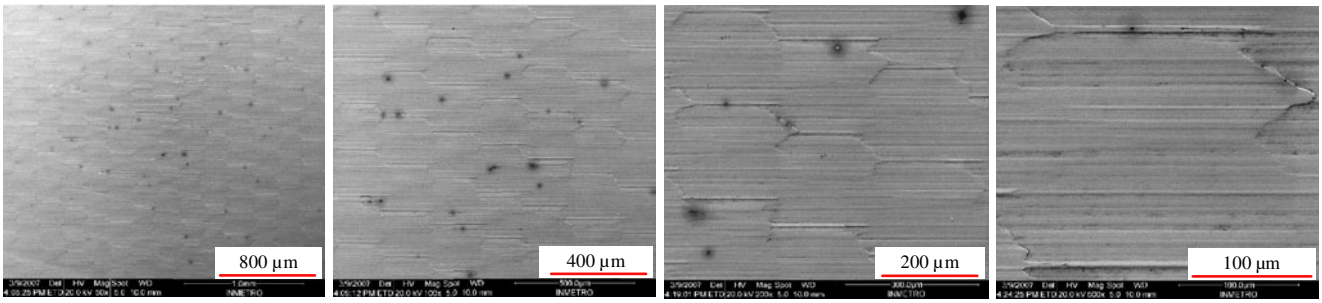

Fig. 8 SEM images for the VD strategy with magnifications (*left* to *right*) of 50×, 100×, 200×, and 500×

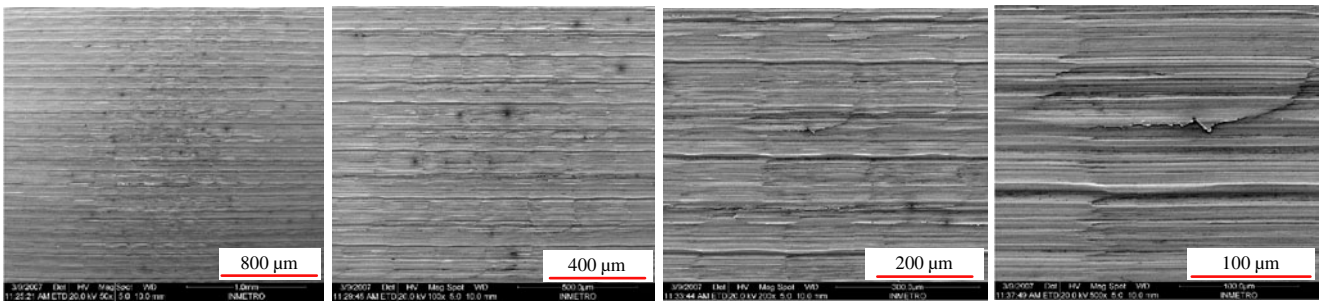

Fig. 9 SEM images for the HU strategy with magnifications (*left* to *right*) of 50×, 100×, 200×, and 500×

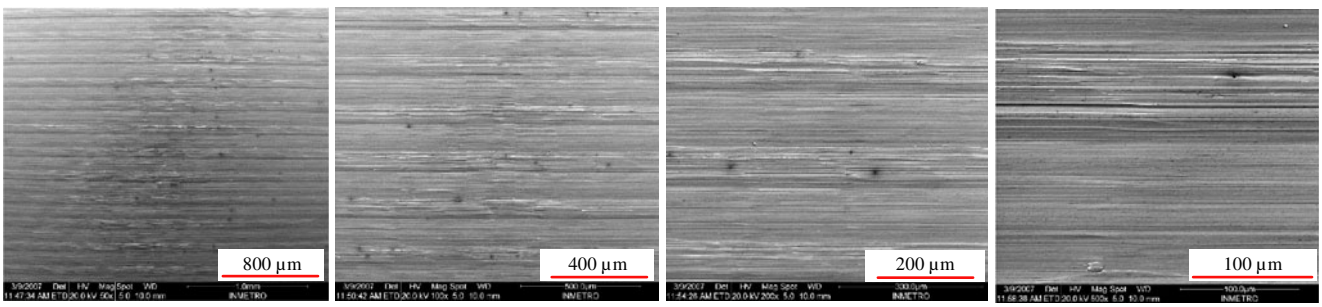

Fig. 10 SEM images for the HD strategy with magnifications (*left* to *right*) of 50×, 100×, 200×, and 500×

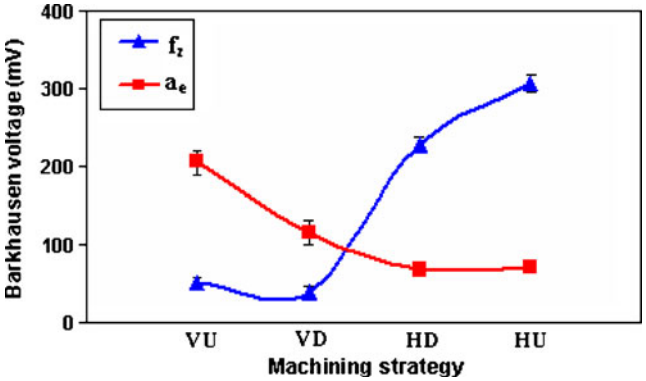

Fig. 11 Average values of MBN along (f_z) and transverse (a_e) to tool feed (color online)

correlation between MBN amplitude and material cutting direction indicates the presence of sub-surface modifications, even though it is not possible to establish a correlation with values of surface roughness.

These MBN results led us to perform a metallographic analysis to look for possible sub-surface modifications. From this analysis, it was possible to observe plastic deformation in a direction normal to tool feed (a_e) for the VU and VD strategies, while the observed plastic deformation was along the tool feed (f_z) for the HU and HD strategies. The maximum plastic deformation values encountered are shown in Fig. 12.

As can be seen by comparing Figs. 11 and 12, the observed plastic deformation follows the same general pattern as was observed for the MBN. One observes plastic deformation in the sub-surface region in the direction of the cutting motion, which also results in elevated values of the MBN. On the other hand, sub-surface plastic deformation was not observed for the VU or VD strategies along the direction of tool feed, nor was it found for HU and HD perpendicular to the tool advance. (It was not possible to establish a relation between sub-surface plastic deformation and surface roughness, and we observed distinct sub-surface deformations for similar values of the roughness.) These observations are perfectly consistent and plausible.

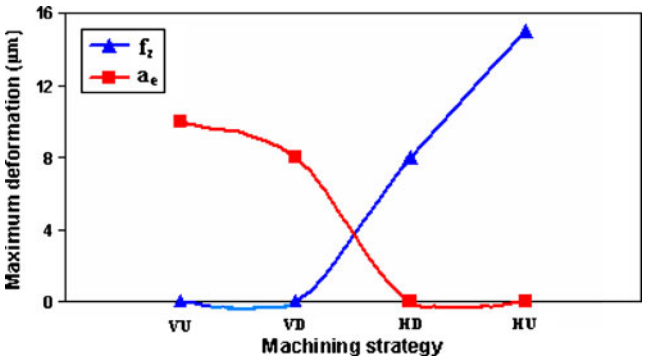

Fig. 12 Maximum plastic deformation along (f_z) and normal (a_e) to tool feed for the strategies considered (color online)

As for residual stress, it is known that residual stresses are the result of inhomogeneous plastic deformation and/or volume changes associated with phase transformations. See Brinksmeier et al. [12]. A simple model suggests that surfaces generated by a cutting operation without a following squeezing have tensile stresses, while surfaces that are squeezed and thus plastically deformed after the cutting process have compressive stresses. Heat production during machining tends to take the residual stresses towards the tensile direction. The stresses in our workpiece are very much a function of the tool geometry and the general conditions of our experiment. Since the milling operations studied here were performed without cutting fluid, it is very probable that the stresses in our workpieces are tensile. Since the MBN data provide a relative measurement of residual stresses, it would be necessary to perform x-ray diffraction measurements to determine the sign of the stresses produced in our workpieces. We have, however, verified a substantial modification of the sub-surface region due to the milling process. The induced stresses in this region are consistent with machining geometry.

4 Conclusions

Our results clearly illustrate that using a VU cutting path orientation gave the highest surface roughness. This machined surface presents the worst surface finish, as well as an irregular texture with material side flow. For this strategy, we suggest that adhesive wear may be coupled with a heavy plastic deformation under the extremely severe conditions that occur between the cutting edge of the tool and the machined surface. The VD cutting path orientation gave the lowest surface roughness and best workpiece surface texture. This strategy gave rise to a well-defined surface with regular cutter marks. This machined surface texture seems to be relatively isotropic.

We initiated an investigation of the sub-surface region using MBN together with an optical analysis to verify the presence of plastic deformation in the sub-surface region. We consistently found that measured values of MBN were larger along the directions where elevated degrees of plastic deformation are found in the sub-surface region.

Acknowledgements The authors wish to acknowledge the financial support of the Brazilian agency CNPq. The authors would like to thank Taeko Y. Fukuhara from INMETRO for the technical support as well as ARWI *Representações Comerciais Ltda.*—authorized Dealer Sandvik Coromant—for the technical and material support. We are also grateful to the staff of the Machining Group of the University of Caxias do Sul, whose contribution was essential to the development of this study.

References

1. Junz Wang JJ, Zheng MY (2003) On the machining characteristics of H13 tool steel in different hardness states in ball end milling. Int J Adv Manuf Technol 22:855–863
2. Bet L (1999) Estudo da Medição da Textura de Superfícies Com Sondas Mecânicas e Sondas Ópticas Tipo Seguidor. Ph.D. Thesis (Mechanical Engineering) Universidade Federal de Santa Catarina. (in Portuguese)
3. Tabenkin A (2005) Surface finish: a machinist's tool, a design necessity. Mod Mach Shop. Nº 3. 30 May www.mmsonline.com
4. Chen JS, Huang YK, Chen MS (2005) A study of the surface scallop generating mechanism in the ball-end milling process. Int J Mach Tools Manuf 45:1077–1084
5. Kang MC, Kim KK, Lee DW, Kim JS, Kim NK (2001) Characteristics of inclined planes according to the variations of cutting direction in high-speed ball-end milling. Int J Adv Manuf Technol 17:323–329
6. Toh CK (2004) Surface topography analysis in high speed finish milling inclined hardened steel. Precis Eng 28:386–398
7. Ng E-G, Lee DW, Dewes RC, Aspinwall DK (2000) Experimental evaluation of cutter orientation when ball nose end milling Inconel 718™. J Manuf Process 2:108–115
8. Tonshoff HK, Camacho JH (1989) Die manufacturing by 5- and 3-axes milling. J Mech Work Technol 20:105–119
9. Fuller KNG, Tabor D (1975) The effect of surface roughness on the adhesion of elastic solids. Proc R Soc Lond 345:327–342
10. Stachowiak GW, Batchelor AW (2001) Engineering tribology, 2nd edn. Butterworth, Heinemann
11. Buttle DJ, Moorthy V, Shaw B, Lord JD (2006) Determination of residual stresses by magnetic methods. NPL Meas Good Pract Guide No. 88. ISSN: 1368-6550
12. Brinksmeier E, Cammett JT, König W, Leskovar P, Peters J, Tönshoff HK (1982) Residual stresses — Measurement and causes in machining processes. Ann CIRP 31(2):491–510